Supramolecular Gel Control of Cisplatin Crystallization: Identification of a New Solvate Form using a Cisplatin-Mimetic Gelator†

Arnab Dawn,* Katherine S. Andrew, Dmitry S. Yufit, Yuexian Hong, J. Prakasha Reddy, Christopher D. Jones, Juan A. Aguilar and Jonathan W. Steed*

Department of Chemistry, Durham University, South Road, Durham DH1 3LE, UK

ABSTRACT: A series of platinum based low molecular weight urea-based gelators **C1**, **C2** and **C3**, mimicking the structure of the anticancer drug cisplatin has been synthesized, as part of the development of a targeted, supramolecular gel phase crystallization and polymorphism screening strategy. Morphological and rheological studies established that inclusion of a longer spacer between the urea and cisplatin-mimetic regions of the gelator (**C3**) resulted in optimal gelation performance. Interfacial crystallization of cisplatin in a gel-sol biphasic system has been employed to address the insolubility of the drug molecule in organic solvents. A new *N*,*N*-dimethylacetamide (DMA) solvate of cisplatin has been identified and a crystal habit modification of the known *N*,*N*-dimethylformamide (DMF) solvate form of cisplatin has been observed on crystallization of cisplatin in **C3** gels prepared in xylenes. While both targeted and non-targeted gels resulted in the formation of the new DMA solvate, only the targeted **C3** gel resulted in high quality single crystal suitable for characterization by single crystal crystallography. The high crystal quality is attributed to a close match between the core geometry of **C3** with that of cisplatin together with local order in the gel fibers of **C3**.

INTRODUCTION

Polymorphism and the methods used to discover drug solid forms are key issues in the pharmaceutical industry, drawing huge intellectual and financial investment.[1] Different crystal forms (polymorphs, pseudopolymorphs, salts or cocrystals) have different bioavailability and solubility, while crystal morphology significantly affects processing and tableting behaviour.[1,2,3] The pharmaceutical industry has adopted extensive solid form screening protocols in order to ensure the identification of all polymorphic and solvate forms of new drug entities. However, the case of ritonavir illustrates that the nucleation of even the most stable polymorphic modification can be difficult, particularly if the conformation in the crystal is different to the form in solution.[4] While the use of a metastable or solvate crystal in a pharmaceutical dosage form can sometimes be justified because a medical benefit is achieved,[5] it is vital from a regulatory standpoint that a thorough characterization of the solid state chemistry of a new drug substance is achieved and all possible forms are identified.[6] In addition to polymorphic form, the external morphology of a crystalline material can be important, with a number of examples demonstrate the effects of changing morphology on *in vitro* dissolution rate, with potential for improving the bioavailability.[7] Thus, there remains a demand for novel, modern polymorph screening technologies which can extend the solid form nucleation and growth parameter space, particularly for hard-to-nucleate solid forms.

As an alternative to solution-based methods, growing crystals from aqueous silica gel or aqueous biogels is a well-established technique.[8] Very recently, an approach based on self-assembled fibers of low molecular weight gelators[9] (LMWGs) has emerged as a chemically diverse, reversible and synthetically tuneable alternative to traditional gel media.[10] However, the potential of supramolecular gels as a medium for crystal growth remains largely unexplored,[11] with the exception of some interesting work on inorganic crystal growth as part of studies on biomineralisation.[12] In 2010 our group demonstrated for the first time that the crystals of several model pharmaceutical compounds can be grown in supramolecular gels in a variety of solvents.[13] However, the gelators used in this study were generic in nature and lacked specific interaction with the drug molecules. A more fine-tuned approach would involve chemically targeting the structure of the gelator in terms of molecular geometry and functional groups to match that of the drug substance hence offering the possibility of a lowered nucleation barrier or even epitaxial overgrowth of the drug substance on the locally ordered gel fibers.

The role of a gel in a crystallization process is slowing down the diffusion of substrates, eliminating convection and providing homogeneous medium for nucleation free of active surfaces such as glass or dust.[11,14] A classical gel phase crystallization therefore involves very slow diffusion of two reactants together in a gel to produce an insoluble product that deposits in the gel medium. However, the local one-dimensional ordering of gel fibers potentially offers an active, surface on which substrate nucleation can occur in such a way that the periodicity of the gel fiber underlies, and is transferred to the growing crystal in a process of heterogeneous secondary nucleation.

Scheme 1: Preparation of cisplatin-mimetic gelators

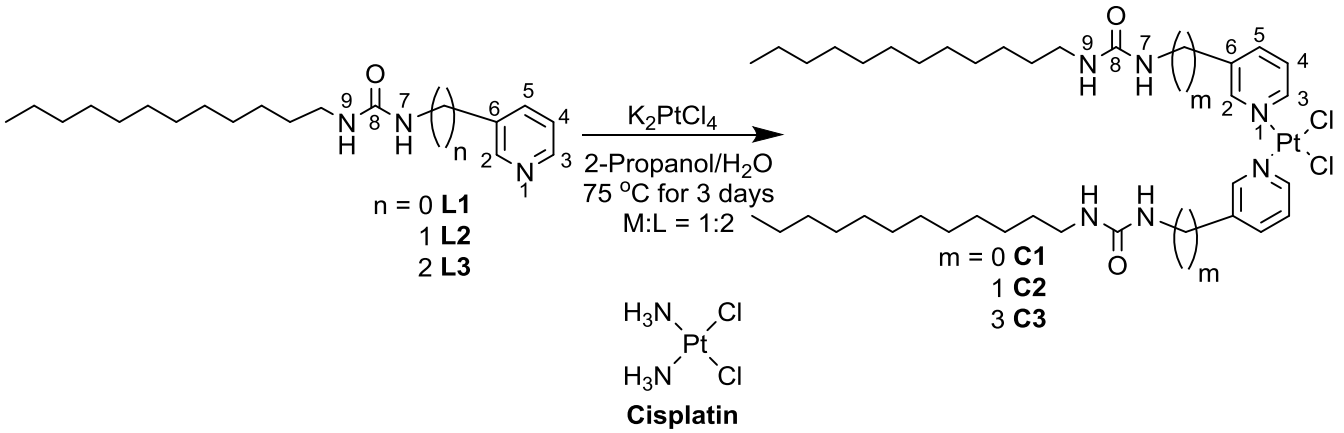

This kind of growth of a daughter phase on a parent substrate was responsible, for example, for the recent isolation of a computationally predicted catameric carbamazepine form V by growth on a dihydrocarbamazepine (DHC) form II parent phase..[15] Herein, we report for the first time, the use of a drug-mimetic LMWG as a template for the growth of a specific drug, namely cisplatin, an important and clinically approved chemotherapeutic drug used for the treatment of testicular and ovarian cancers.[16]

Cisplatin is structurally simple and its polymorphism is well-established; it represents a case where there is considerable confidence that no hitherto undiscovered forms exist. The first published crystal structure of cisplatin was the low resolution determination of the alpha form reported five decades ago,[17] while the beta form was reported in the patent literature.[18] Only recently, has detailed structural information for these two pure forms has been reported with the help of single crystal X-ray and neutron powder diffraction experiments.[19] There are also two known polymorphs of a solvate form of cisplatin containing *N*,*N*-dimethylformamide (DMF),[20] a DMF solvated complex with [18]crown-6,[21] and a remarkable metallocage cisplatin inclusion compound.[22] The presence of only a limited number of functional groups (which makes the molecule insoluble in most organic solvents), together with the presence of the relatively labile chloro ligands (which undergo exchange with water as part of the drug's mode of action) leaves only limited scope for further polymorphism and hence offers a challenging test case for novel solid form screening methodologies.

In the present work we have prepared a series of cisplatin-mimetic metal complexes **C1**, **C2** and **C3**, involving a cis-dichloro platinum(II) linker bound to the respective pyridine-based ligands **L1**, **L2** and **L3** (Scheme 1). These metal-bridged bis(urea) metallogelators have the potential to form gels based on the self-assembly of the urea functional groups,[23,24] while the dodecyl chains enhance the solubility in organic solvents, and at the same time participate in strong van der Waals interactions, facilitating the formation of fibrous networks. With the exception of one earlier report of a silver(I) coordinated mono urea based gel system,[25] the use of a metal center to link two urea-based ligands to give a gel-forming bis(urea) motif by metal complexation has not been reported. It represents a simple and highly versatile approach to the preparation of a range of bis(urea)s as well as incorporating *inter alia* the target cisplatin-mimetic functionality. The variability of the pyridyl-urea spacer group offers the scope to investigate the effect of relative distance between the coordinating segment and self-assembling segment on the overall gelation and templating behavior of the system.

The novelty of this work lies in three key elements: firstly, the concept of linking two monoureas together using a metal-ligand strategy facilitating the gel formation and secondly, the design of a specific drug-mimetic gel as an example of an advanced pharmaceutical crystallization strategy for solid form discovery. Thirdly, the work also reports a new gel-sol interfacial crystallization technique to address the different solubilities of the drug and gelator.

RESULTS AND DISCUSSION

Synthesis of Cisplatin-Mimetic Gelators. Gelators **C1**, **C2** and **C3** were prepared from the reaction of respective ligands **L1**, **L2** and **L3** with potassium tetrachloroplatinate(II) in a 2-propanol/water mixture at 75 °C for 3 days. Final purification was carried out by column chromatography. Gelators were characterized by ^{1}H, ^{13}C, ^{195}Pt NMR spectroscopy and spectra were assigned with the aid of ^{1}H-^{1}H gCOSY, ^{1}H-^{13}C gHSQC, ^{1}H-^{13}C gHMBC, ^{1}H-^{15}N gHMBC in DMF-d_7 solution at 298 K. Table 1 summarizes key chemical shifts changes on coordination. The pyridine nitrogen atom N1 was identified unambiguously as the coordination site by ^{1}H-^{15}N gHMBC, where a large chemical shift change for N1 was observed for all the complexes compared to only a negligible chemical shift change for N7 and N9 associated with the urea moiety (Scheme 1). As expected, the hydrogen atoms adjacent to N1 experienced significant downfield shifts upon complexation. The hydrogen atom attached to N7 in **C1** also experiences a large downfield shift reflecting its proximity to the coordination site.

The ^{195}Pt NMR resonances for all three complexes lie in the same range implying a similar environment for the Pt(II) centers in each case. The ^{195}Pt NMR signals for complexes of this type vary significantly depending on the ligand type, geometry (*cis*-/*trans*-) and the solvent.[26]

Table 1. ^{1}H, ^{13}C, ^{15}N differential chemical shifts ($\delta_{Complex}$ - δ_{Ligand}, in ppm) upon complexation and ^{195}Pt chemical shifts (in ppm) as observed for the complexes ('w' represents a weak signal)

Complex	^{1}H NMR				^{13}C NMR		^{1}H-^{15}N gHMBC			^{195}Pt
	C2H	C3H	N7H	N9H	C2	C3	N1	N7	N9	
C1	0.36	0.17	0.39	0.18	2.53	2.83	138.4	1.40	1.50	-1962.53 -1941.79 (w)
C2	0.28	0.3	0.17	0.14	3.37	3.79	132.33	-1.49	0.38	-1960.64
C3	0.29	0.29	0.12	0.01	3.22	3.87	132.18	-0.77	-0.01	-1960.36

Table 2. Raman frequencies for complexes C1 – C3 (663 nm laser, 'sh' indicates a shoulder)

	C1	C2	C3
Pt-Cl stretching	322 (sh), 325.7	324.5, 329.5	324.5, 329.5

Generally, pyridyl complexes resonate at lower field than their amine analogues because of the weaker basicity of the pyridine ligand. The appearance of single signal in the ^{195}Pt NMR spectra of **C2** and **C3** implies a single isomeric form of the complexes. For **C1** a second weak signal was observed indicating the possible presence of a small amount of the *trans* isomer. The *cis* isomeric form is a crucial aspect of the gelator design. As chloride has a greater *trans* effect than pyridyl ligands, the synthetic route is expected to favor the *cis* geometry.[27] However the difference between chloride and pyridyl ligands is relatively small in terms of *trans* effect, and hence we examined the complexes by Raman spectroscopy to confirm isomeric form. The *cis* form of the complexes has C_{2v} symmetry and thus both symmetric and antisymmetric Pt-Cl stretching vibrations are Raman active. The *trans* isomers are D_{2h} and only the symmetric Pt-Cl stretching is Raman active. As summarized in Table 2, **C2** and **C3** clearly showed two bands, while a peak with a shoulder was observed for **C1**. These results confirm a *cis* geometry for **C2** and **C3**, and suggest a small fraction of *trans* form in case of **C1.**

Preparation and Characterization of the Gel Samples. The gelation behaviors of **C1**, **C2** and **C3** were tested in a variety of organic solvents by dissolving the solid samples at a high temperature followed by cooling to room temperature. Gelation was evaluated by the simple 'stable to inversion' test. **C1** and **C3** behaved similarly and form gels in xylenes (*o*-, *m*- and *p*-), toluene and chloroform. On the other hand, **C2** formed gels in a series of alcohols (Supporting Information Table S1).

The morphologies of the xerogel samples vary from fibril-like to ribbon-like to well-defined fibrils for **C1**, **C2** and **C3**, respectively, as studied by scanning electron microscopy (SEM) (Figure 1 and Supporting Information Figure S22). This variation is also reflected in rheology of the samples. While **C2** exhibited the highest value of the storage modulus at 2.5% w/v, gels of **C3** showed the highest yield stress (Figure 2).

Formation of the assembled fibers driven by intermolecular hydrogen bonding of the bis(urea) moieties is evidenced by the temperature dependent NMR spectra of complexes **C1** and **C3** in deuterated chloroform, a gel-forming solvent (Supporting Information Figure S23-S24).[28] The urea hydrogen atoms (attached to N7 and N9) in **C3** exhibited a marked up-field shift in at higher temperature even at high dilution, which is characteristic of hydrogen bond based assembly.[29] Interestingly, the hydrogen atoms attached to the urea group N7 and N9 in **C1** responded differently to the temperature change. While the latter shifted up-field, the former showed the opposite behavior with increasing temperatures. This behavior is attributed to the conformational rigidity associated with the direct attachment of the urea moiety to the coordinating site, preventing optimum hydrogen bonding interactions. The van der Waals interactions among the dodecyl chains are also expected to play an important role in forming the network structure. Other possible modes of intermolecular interaction include Pt-Pt interaction and π-π interaction via the pyridyl rings. The presence of alkylene spacers in the complexes plays a crucial role in isolating the coordination region and self-assembling region. The square planar geometry of the coordinated platinum center should impose some degree of conformational restriction to the rest of the molecule in achieving a suitable alignment for constructing a one-dimensional assembly. This restriction is most significant in the case of **C1** because of the closest proximity of the coordination and gelation domains. Additionally, direct attachment of the urea moiety to the aromatic ring substantially diminishes the efficiency of hydrogen bond formation in **C1**. On the other hand, the two domains are apparently isolated in **C3**, giving rise to the highest degree of flexibility for the alignment of bis(urea) motifs. The situation of **C2** lies in between those two extremes.

Supramolecular Gel Phase Crystallization of Cisplatin. Gel phase crystallization commonly involves dissolving the LMWG and the substrate in a common solvent under sonication and/or heating to give a homogeneous sol that is then allowed to cool, resulting in rapid gelation followed by crystallization on a slower time scale.[13] However, the insolubility of cisplatin in most organic solvents except DMF means that this strategy is not viable. As a result we adopted a method involving a biphasic gel-sol system, in which a cisplatin solution in DMF was allowed to diffuse into a contiguous gel based on targeted gelators **C1–3** prepared in another suitable solvent (Figure 3). The advantages of this process are two-fold: firstly, simultaneous heating of both the components is not required, therefore minimizing the possibility of chemical reaction between two structurally similar compounds; secondly, it eliminates the necessity of having a common solvent, therefore adding more versatility in terms of solvent selection.

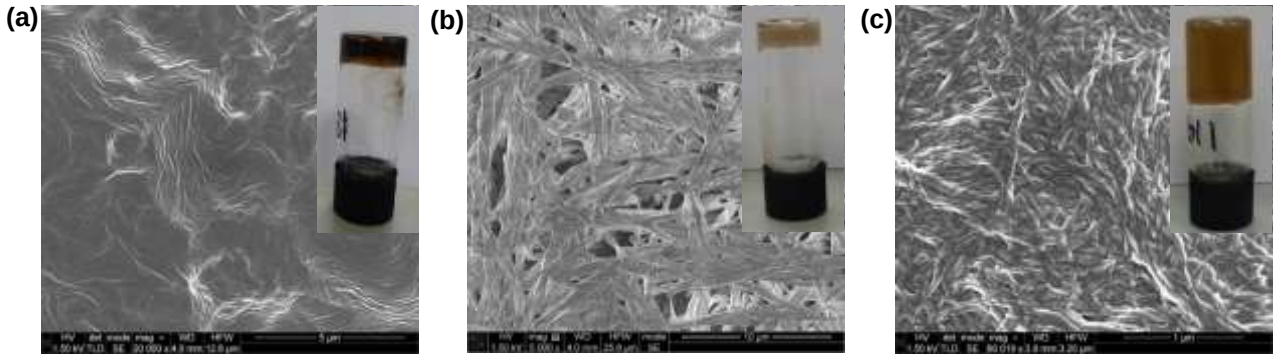

Figure 1. SEM micrographs of the xerogel systems (1.5% w/v): (a) **C1** in toluene, (b) **C2** in 1-propanol and (c) **C3** in toluene. Inset: photographs of the gel samples.

In a typical procedure, a cisplatin solution in DMF (1.5% w/v) was added slowly on the top of a pre-formed gel (2% w/v) prepared in another organic solvent. Gels of **C1** and **C3** in *o*-xylene (*p*- and *m*-xylene gave similar results) produced yellow plate-like crystals. A control experiment in pure DMF did not result in crystal formation under the same conditions. Replacing the targeted gel with *o*-xylene gels of a generic LMWG **G** bearing no structural similarity to cisplatin (Supporting Information Figure S25)[24b] or by replacing the gel with pure *o*-xylene solvent, also generated similar plate-like crystals. Single crystal X-ray diffraction confirmed the crystals as the known triclinic DMF solvate of cisplatin.[20b] Crystallization results are summarized in Table 3. The most interesting finding was the temperature dependence of the crystal morphology observed in the presence of **C3**. While low temperature crystallization in the presence of the **C3** gel and in the control experiments produced yellow plate-like crystals with irregular shapes, room temperature (20 ^{o}C) crystallization in the **C3** gel produced a substantial fraction of yellow hexagonal plate-like crystals in addition to irregular plates. This represents a novel morphology for the cisplatin DMF solvate and could be generated only in the presence of **C3** gels in xylenes near to room temperature. Habit modification may indicate selective adsorption of the gelator on the fastest growing face of the crystals.[30] Interestingly, none of the gels prepared from **C2** (in all gel-forming alcohols) gave cisplatin crystals using the same layering approach, presumably reflecting the more polar solvent. Also, gels prepared from **C1** and **C3** in solvents other than xylenes did not result cisplatin crystals.

Despite its facile formation, the DMF solvate is unstable and rapidly loses DMF upon exposure to atmosphere. This observation prompted us to find an alternative solvent to replace the DMF, despite the lack of other known solvate forms. Cisplatin precipitates immediately from *N*,*N*-diethylformamide (DEF) whereas it is moderately soluble in *N*,*N*-dimethylacetamide (DMA). Interestingly, the same bilayer gel-sol technique using DMA solvent yielded high quality yellow rectangular plate-like single crystals from gels of **C3** in *o*-, *m*- and *p*-xylene. In contrast, control experiments performed in the presence of *o*-xylene gels of either **C1** or **G** produced only a mass of small microcrystals (Figure 4) suggesting an effect of the gel on controlling crystal nucleation frequency. The crystals obtained from the **C3** gel were characterized by single crystal X-ray crystallography and proved to be a new solvate form of cisplatin incorporating one DMA molecule per two cisplatin molecules (Figure 5).[31] This material is only the second known solvate form of cisplatin. The material crystallizes in space group $P\bar{1}$ and has a related channel structure to the triclinic DMF solvate in the same space group. Full crystallographic parameters are given in Tables S2-S9 in the Supporting Information. However, unlike the related triclinic DMF solvate[20b] which has a 1:1 solvent to cisplatin ratio the asymmetric unit has two cisplatin molecules to one DMA (Figure 5a). The solvent molecule is disordered with each atom over two positions with occupancy of 0.75 and 0.25 respectively. The packing arrangement in the crystal is shown in Figure 5b. The two unique cisplatin molecules both have a square planar geometry and are linked through N-H···Cl hydrogen bonding (N···Cl 3.424(5), 3.443(6) Å; N-Ĥ···Cl 171–175^{o}) (Supporting Information Figure S26 and Table S7). The carbonyl group of the DMA molecule interacts with the ammine ligands of the cisplatin via N-H···O hydrogen bonding (N···O 2.889(13) Å, N-Ĥ···O 159^{o}). In addition, close Pt···Pt interactions of 3.205(5) and 3.316(8) Å are also present as observed in other platinum(II) complexes.[17, 20, 32]

The crystalline material from all DMA crystallizations was analyzed by X-ray powder diffraction (XRPD) to assess bulk solid form. The data indicate that the samples are a mixture of varying amounts of the new DMA solvate form and solvent-free cisplatin, identified by fitting to the calculated patterns derived from single crystal data (see supplementary information Figures S27–32).[19,31] There is also evidence for small amounts of an additional unidentified phase. Gels of generic gelator **G** yielded crystals that are predominantly cisplatin DMA solvate with some alpha cisplatin. Gels of **C1** and **C3** gave a mixture of the DMA solvate and both alpha and beta cisplatin. The presence of alpha and beta cisplatin may arise from desolvation of initially formed solvate during the preparation of the sample for XRPD, although concomitant formation of solvate and pure cisplatin forms cannot be ruled out. The data establish that all of the supramolecular gels **G**, **C1** and **C3** are capable of producing the new DMA hemisolvate form of cisplatin. However, the drug-mimic LMWG **C3** produced high quality single crystals suitable for single crystal X-ray diffraction.

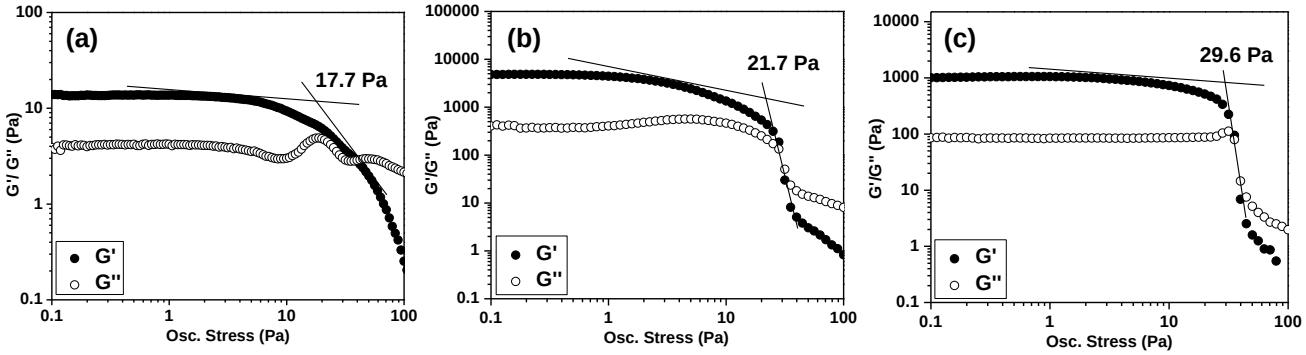

Figure 2. Determination of the linear regime: Measurement of storage and loss moduli as a function of applied stress at a constant angular frequency of 1 Hz, performed at 20 ^{o}C for different gel systems (2.5% w/v): (a) **C1** in toluene, (b) **C2** in 1-propanol and (c) **C3** in toluene.

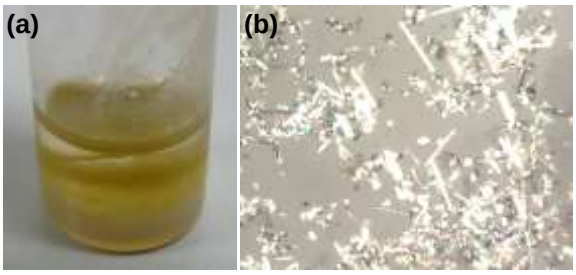

Figure 3. (a) Photo showing the yellow cisplatin crystals grown at the interface of the gel-sol bilayer system consisting of a *o*–xylene gel of **C3** (2% w/v) at the bottom layer and a solution of cisplatin in DMF at the top layer; (b) Optical microscope image (90 times magnification) of the cisplatin crystals grown at the gel-sol interface, at room temperature.

Initial control experiments based on diffusing a DMA solution of cisplatin into *o*-xylene did not result in formation of the DMA solvate phase. However, later control experiments did result in formation of mixtures of the solvate and amorphous material. The size of the DMA solvate crystals from the control system was improved and the amount of amorphous material decreased by undertaking the crystallization at low temperature (4 ^{o}C). Since the new solvate was formed initially in the gels and appeared only in control experiments without the gels some months afterwards it is possible that seeding from the gel-grown sample is a factor in the formation of the DMA solvate.

The thermal stability of the new DMA hemisolvate was analyzed by thermogravimetric analysis. A wet sample obtained from gels of **G** was used in order to avoid any possible interference which might arise from **C3** having similar functional groups as those of cisplatin. The thermogram shows that loss of surface DMA is complete by 63 ^{o}C while included DMA is lost shortly afterwards in a continuous process consistent with the channel nature of the solvate (Figure 6). Elimination of two ammonia ligands takes place in stepwise manner, followed by loss of chlorine.

XRPD patterns of the xerogel samples of **C1** and **C3** prepared from *o*-xylene give distinct maxima in the low angle region (Figure 7) with a particularly sharp feature in the case of **C3**. The d-spacing matches closely with the approximated 'ordered length' up to the first 6 carbons after the urea motif of the extended **C3** gelator suggesting partial dodecyl chain disorder in an extended conformation in the gel state with stacked "$PtCl_2$" units. In contrast the d-spacing obtained from the XRPD data of **C1** proved to be shorter than the calculated length of the molecular axis for an extended conformation based on an ordered length of six methylene units. Direct attachment of urea with the coordinating pyridyl group may introduce a steric barrier preventing an extended conformation in the gel. This difference in the conformational freedom may be linked to the ability of **C3** to produce high quality crystal samples.

CONCLUSIONS

A series of platinum bearing LMWGs **C1**, **C2** and **C3**, mimicking the structure of cisplatin has been prepared. The **C3** gel with its greater separation of urea and ligating groups proved to the most effective gelator. The cisplatin targeted gels were incorporated into a biphasic gel-sol system for crystallization of the highly insoluble cisplatin. An interesting crystal habit modification of the cisplatin triclinic DMF solvate of cisplatin in the presence of only the **C3** gel was observed. A new DMA hemisolvate of cisplatin is produced by both designer and non-specific gels, however the highest quality single crystals were obtained from the targeted **C3** gel under the conditions employed. We suggest that the structural and geometrical resemblance between this gelator and cisplatin together with the relatively ordered assembly in this gel enhance the influence of the **C3** gels on cisplatin crystallization. The mode of interaction between the gelator and substrate may involve a combination of Pt-Pt stacking and ammine-chloride hydrogen bonding interactions. To the best of our knowledge, this is the first evidence for the use of a drug-mimic supramolecular LMWG system in influencing the outcome of a drug crystallization process. The concepts of designer LMWG as part of a biphasic gel-sol diffusion arrangement offer an intriguing new potential tool in pharmaceutical solid form screening.

Table 3. Crystallization of cisplatin studied in gel-sol bilayer systems, where cisplatin dissolved in DMF constitutes the top layer and various systems as described below form the bottom layer, including a control experiment without a bottom layer.

	o–xylene gel of **C3**		*o*–xylene gel of **C1**		*o*-xylene gel of **G**	*o*–xylene	None
Temperature (^oC)	10	20	10	20	20	20	
Crystal form	DMF solvate	DMF solvate	DMF solvate	DMF solvate	DMF solvate	DMF solvate	No crystal
Morphology[a]							

[a] Photographs of the crystals as mounted for single crystal X-ray study

EXPERIMENTAL SECTION

Materials. Cisplatin was purchased from TCI and was established to be beta-cisplatin by XRPD (see supplementary information, Figure S29). Ligands **L1**, **L2** and **L3** were prepared from the reaction of pyridyl amines with dodecyl isocyanate. In a typical procedure, the amine (1 equivalent) was dissolved in dry dichloromethane. The solution was cooled to 0 ^oC and dodecyl isocyanate (1.2 equivalents) dissolved in dichloromethane was added to the reaction mixture drop wise using an addition funnel, under the nitrogen atmosphere. The reaction mixture was allowed to warm to room temperature followed by reflux overnight. Products were collected and purified as described below.

1-dodecyl-3-(pyridin-3-yl)urea (**L1**). 3-aminopyridine (0.5 g, 5.31 mmol) reacted with dodecyl isocyanate (1.35 g, 6.40 mmol).The solvent was removed *in vacuo* and the crude product was recrystallised from ethanol at 0 ^oC to give a white powder (1.22 g, yield 75%).

^{1}H NMR (400 MHz, DMF-d_7): δ 8.90 (1H, s, Ar-N*H*), 8.80 (1H, s, Ar*H*), 8.29 (1H, d, *J* = 4.6 Hz, Ar*H*), 8.17 (1H, d, *J* = 2.6 Hz, Ar*H*), 7.41 (1H, dd, *J* = 4.7, 4.3 Hz, Ar*H*), 6.52 (1H, t, *J* = 5.6, -N*H*$C_{12}H_{25}$), 3.35 (2H, q, *J* = 6.8 Hz, -C$H_2C_{11}H_{23}$) , 1.67 (2H, quin, *J* = 7.1 Hz, -C$H_2C_{10}H_{21}$), 1.43 (18H, m, -$CH_2C_9H_{18}CH_3$), 1.03 (3H, t, *J* = 6.8 Hz, -CH_3); ^{13}C{^{1}H} NMR (151 MHz, DMF-d_7): δ 155.71, 142.36, 140.01, 138.06, 124.50, 123.55, 39.73, 31.95, 30.35, 29.72, 29.69, 29.45, 26.97, 22.66, 13.83; FT-IR (ν_{max}/cm^{-1}): 3339, 3041, 2955, 2917, 2850, 1673, 1651, 1558; Anal. calcd for $C_{18}H_{31}N_3O$: C 70.78, H 10.23, N 13.76, found C 70.72, H 10.21, N 13.65; MS (ESI): m/z calcd 306.2, found 306.2 $[M+H]^+$.

1-dodecyl-3-((pyridin-3-yl)methyl)urea (**L2**). 3-picolylamine (0.5 g, 4.62 mmol) reacated with dodecyl isocyanate (1.17 g, 5.55 mmol). The reaction mixture was allowed to cool at room temperature and the precipitate was collected by filtration to give a white powder (1.25 g, yield 85%).

^{1}H NMR (400 MHz, DMF-d_7): δ 8.73 (1H, s, Ar*H*), 8.63 (1H, d, *J* = 4.8 Hz, Ar*H*), 7.89 (1H, d, *J* = 7.8 Hz, Ar*H*), 7.52 (1H, dd, *J* = 4.8 Hz, Ar*H*), 6.65 (1H, t, *J* = 5.8 Hz, $ArCH_2NH$), 6.29 (1H, t, *J* = 5.6 Hz, -N*H*$C_{12}H_{25}$), 4.54 (2H, d, *J* = 6.1 Hz, $ArCH_2$-), 3.31 (2H, q, *J* = 6.8 Hz, -C$H_2C_{11}H_{23}$), 1.63 (2H, quin, *J* = 6.7 Hz, -C$H_2C_{10}H_{21}$), 1.46 (18H, m, -$CH_2C_9H_{18}CH_3$), 1.06 (3H, t, *J* = 6.9 Hz, -CH_3); ^{13}C{^{1}H} NMR (151 MHz, DMF-d_7): δ 158.65, 149.22, 148.20, 137.16, 135.03, 123.50, 41.20, 40.00, 31.96, 30.67, 29.73, 29.50, 27.01, 22.67, 13.84; FT-IR (ν_{max}/cm^{-1}): 3346, 3313, 3037, 2960, 2921, 2849, 1615, 1569; Anal. calcd. for $C_{19}H_{33}N_3O$: C 71.43, H 10.41, N 13.15, found C 71.35, H 10.37, N 13.09; MS (ESI): m/z calcd. 320.2, found 320.1 $[M+H]^+$.

1-dodecyl-3-(2-(pyridin-3-yl)ethyl)urea (**L3**). 3-(2-aminoethyl)pyridine (0.5 g, 4.1 mmol) reacted with dodecyl isocyanate (1.04 g, 4.92 mmol). The solvent was removed *in vacuo* and the crude product was purified by column chromatography [silica gel, $CHCl_3$/ MeOH = 15:1 (v/v)] to give yellowish white powder (1.06 g, yield 78%).

^{1}H NMR (400 MHz, DMF-d_7): δ 8.65 (1H, s, Ar*H*), 8.63 (1H, d, *J* = 4.9 Hz, Ar*H*), 7.83 (1H, d, *J* = 7.8 Hz, Ar*H*), 7.52 (1H, dd, *J* = 4.8 Hz, Ar*H*), 6.12 (2H, br, -CH_2N*H*CON*H*CH_2-), 3.56 (2H, q, *J* = 6.7 Hz, $ArCH_2CH_2NH$-), 3.26 (2H, q, *J* = 6.8 Hz, -NHC$H_2C_{11}H_{23}$), 2.96 (2H, t, *J* = 7.0 Hz, $ArCH_2CH_2$-), 1.60 (2H, quin, *J* = 6.6 Hz, -C$H_2C_{10}H_{21}$), 1.46 (18H, m, -$CH_2C_9H_{18}CH_3$), 1.06 (3H, t, *J* = 6.8 Hz, -CH_3); ^{13}C{^{1}H} NMR (151 MHz, DMF-d_7) δ 158.56, 150.46, 147.70, 136.33, 135.78, 123.57, 41.14, 39.86, 33.83, 31.96, 30.70, 29.74, 29.70, 29.50, 27.02, 22.67, 13.84; FT-IR (ν_{max}/cm^{-1}): 3338, 3313, 3033, 2955, 2922, 2849, 1615, 1571; Anal. calcd. for $C_{20}H_{35}N_3O$: C 72.03, H 10.58, N 12.60, found C 72.05, H 10.56, N 12.55; MS (ESI): m/z calcd. 334.2, found 334.1 $[M+H]^+$.

Synthesis of C1, C2, C3. A hot aqueous solution of potassium tetrachloroplatinate was added to the hot ligand solution in 2-propanol (2-propanol: water = 2:1, v/v) and then the reaction mixture was refluxed at 75 ^oC for 3 days then allowed to cool at room temperature. The resulting precipitate was filtered and washed with hot and cold 2-propanol, and hot and cold distilled water. The crude product was purified by column chromatography [silica gel, $CHCl_3$: MeOH = 20:1 (v/v)] to give a beige powder.

Dichloro-bis(1-dodecyl-3-(pyridin-3-yl)urea)platinum (II) (**C1**). Ligand **L1** (0.23 g, 0.76 mmol) reacted with potassium tetrachloroplatinate (0.16 g, 0.38 mmol) to give **C1** (0.15 g, yield 45%)

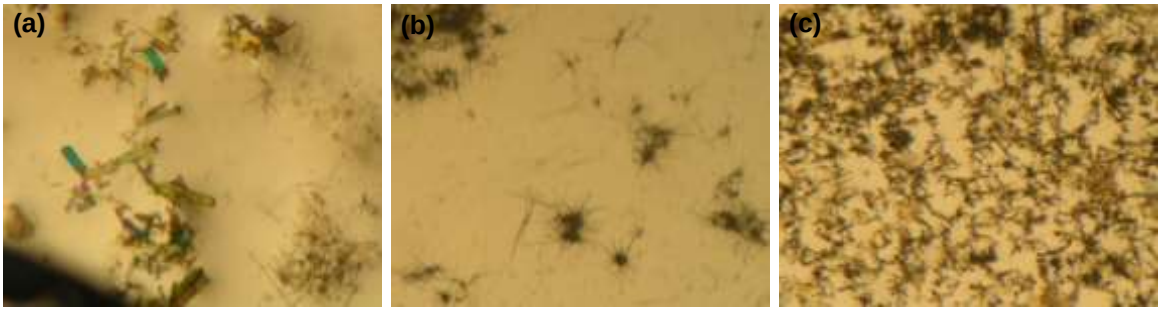

Figure 4. Optical microscope images (90 times magnification) of cisplatin crystals grown in the presence of different gel systems prepared in *o*-xylene (2% w/v): (a) **C3** (b) **C1** and (c) **G**.

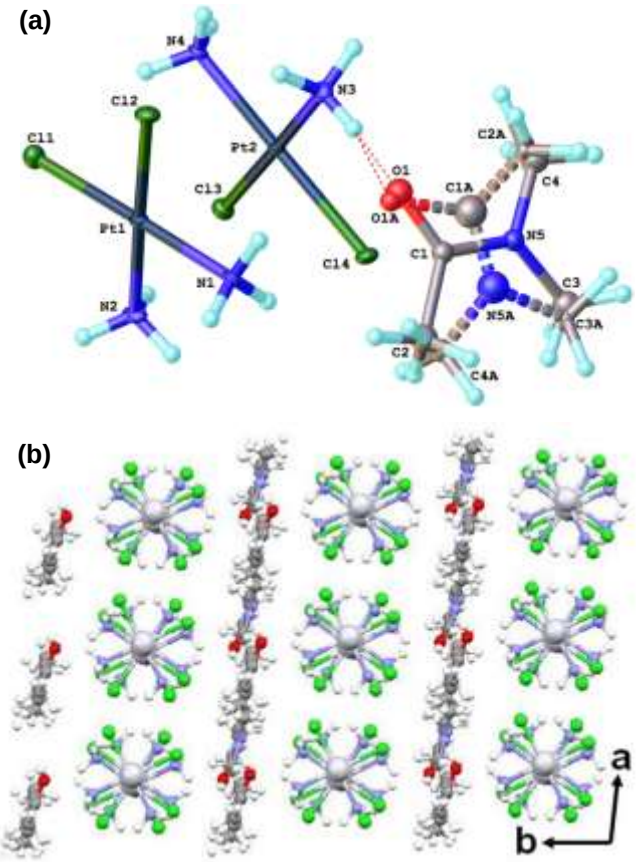

Figure 5. (a) A View of the asymmetric unit of cisplatin DMA solvate showing the atom numbering scheme and (b) packing diagram of the cisplatin DMA solvate viewed along the *c* axis.

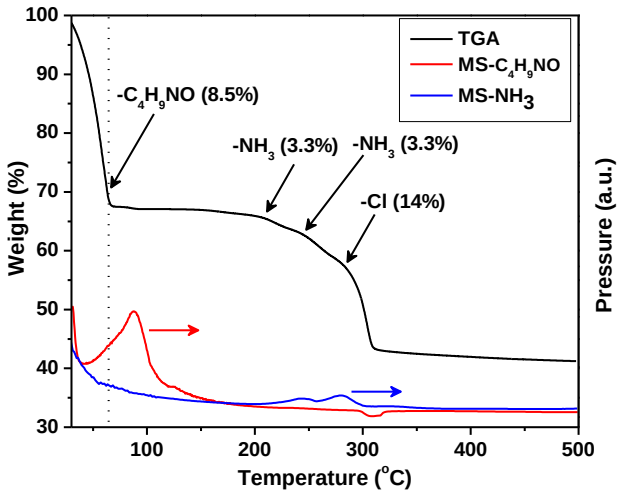

Figure 6. TGA-MS thermograms of cisplatin sample collected from **G** (a small but constant time lag is involved in the mass analysis). The region on the left of the dotted line approximates the elimination of 'free solvent' from the wet system. The black arrows indicate the points of elimination of the included solvent and ligands. The mass calculation of the different components was based on the formula $2PtCl_2(NH_3)_2.C_4H_9NO$ staring from the conclusion of surface solvent loss at 67.5 wt%. The elimination of Cl was assigned based on the residual mass of Pt.

^{1}H NMR (400 MHz, DMF-d_7): δ 9.37 (0.4 H, s, Ar*H*), 9.29 (2H, s, ArN*H*-), 9.16 (1.6 H, s, Ar*H*), 8.57 (0.4 H, d, *J* = 5.3Hz, Ar*H*), 8.46 (1.6 H, d, *J* = 5.3 Ar*H*), 8.31 (1.6 H, d, *J* = 8.4 Hz, Ar*H*), 8.21 (0.5 H, br Ar*H*), 7.53 (2H, dd, *J* = 5.7 Hz, Ar*H*), 6.70 (2H, t, *J* = 5.5 Hz, -N*H*$C_{12}H_{25}$), 3.33 (4H, q, *J* = 6.2 Hz, -C*H*$_2C_{11}H_{23}$), 1.66 (4H, quin, *J* = 6.7 Hz, -C*H*$_2C_{10}H_{21}$), 1.43 (36H, m, -CH_2C_9*H*$_{18}CH_3$), 1.03 (6H, t, *J* = 6.8 Hz, -C*H*$_3$); ^{13}C{^{1}H} NMR (151 MHz, DMF-d_7) δ 155.09, 146.10, 145.19, 143.61, 142.54, 140.13, 139.31, 126.96, 126.18, 125.25, 39.81, 31.94, 30.17, 29.72, 29.40, 29.38, 26.95, 22.65, 13.84; FT-IR (ν_{max}/cm^{-1}): 3359, 3300, 2953, 2920, 2848, 1638, 1554; Anal. calcd. for $C_{36}H_{62}Cl_2N_6O_2Pt$: C 49.31, H 7.13, N 9.58, found C 49.11, H 7.08, N 9.54; MS (MALDI): *m/z* calcd. 899.0, found 899.4 $[M+Na]^+$.

Dichloro-bis(1-dodecyl-3-((pyridin-3-yl)methyl)urea)platinum (II) (**C2**). Ligand **L2** (0.46 g, 1.44 mmol) reacted with potassium tetrachloroplatinate (0.3g, 0.72 mmol) to give **C2** (0.42 g, yield 64%). ^{1}H NMR (400 MHz, DMF-d_7): δ 9.01(2H, s, Ar*H*), 8.93 (2H, d, *J* = 5.8 Hz, Ar*H*), 8.14 (2H, d, *J* = 7.8 Hz, Ar*H*), 7.70 (2H, dd, *J* = 5.8 Hz, Ar*H*), 6.82 (2H, t, *J* = 6.0 Hz, $ArCH_2$N*H*-), 6.43 (2H, t, *J* = 5.7 Hz, -N*H*$C_{12}H_{25}$), 4.60 (4H, d, *J* = 6.0 Hz, ArCH_2-), 3.31 (4H, q, *J* = 6.8 Hz, -C*H*$_2C_{11}H_{23}$), 1.65 (4H, quin, *J* = 6.8 Hz, -C*H*$_2C_{10}H_{21}$), 1.45 (36H, m, -CH_2C_9*H*$_{18}CH_3$), 1.06 (6H, t, *J* = 7.0 Hz, -C*H*$_3$); ^{13}C{^{1}H} NMR (151 MHz, DMF-d_7) δ 158.58, 152.59, 151.99, 139.86,

138.34, 125.36, 40.77, 40.10, 31.97, 29.75, 27.06, 22.68, 13.85; FT-IR (ν_{max}/cm^{-1}): 3348, 3304, 3045, 2953, 2921, 2848, 1624, 1577; Anal. calcd. for $C_{38}H_{66}Cl_2N_6O_2Pt$: C 50.43, H 7.35, N 9.29, found C 50.23, H 7.31, N 9.27; MS (MALDI): *m/z* calcd. 927.0, found 927.4 $[M+Na]^+$.

Dichloro-bis(1-dodecyl-3-(2-(pyridin-3-yl)ethyl)urea)platinum (II) (**C3**). Ligand **L3** (0.32 g, 0.96 mmol) reacted with potassium tetrachloroplatinate (0.2 g, 0.48 mmol) to give **C3** (0.18 g, yield 40%). ^{1}H NMR (400 MHz, DMF-d_7): δ 8.94 (4H, m, Ar*H*), 8.11 (2H, d, *J* = 7.8 Ar*H*), 7.70 (2H, dd, *J* = 5.8 Ar*H*), 6.24 (2H, t, *J* = 5.7 Hz, $ArCH_2CH_2N\mathit{H}$-), 6.13 (2H, t, *J* = 5.6 Hz, -$N\mathit{H}C_{12}H_{25}$), 3.59 (4H, q, *J* = 6.8 Hz, $ArCH_2C\mathit{H}_2$-), 3.28 (4H, q, *J* = 6.6 Hz, -$NHC\mathit{H}_2C_{11}H_{23}$), 3.07 (4H, t, *J* = 7.0 Hz, $ArC\mathit{H}_2$-), 1.63 (4H, quin, *J* = 6.6 Hz, -$C\mathit{H}_2C_{10}H_{21}$), 1.46 (36H, m, -$CH_2C_9\mathit{H}_{18}CH_3$), 1.06 (6H, t, *J* = 6.7 Hz, -$C\mathit{H}_3$); ^{13}C{^{1}H} NMR (151 MHz, DMF-d_7): δ 158.56, 153.68, 151.57, 139.74, 138.23, 125.39, 40.74, 39.93, 33.50, 31.96, 30.69, 29.74, 27.06, 22.67, 13.84; FT-IR (ν_{max}/cm^{-1}): 3340, 3315, 3037, 2956, 2922, 2849, 1614, 1574; Anal. calcd. for $C_{40}H_{70}Cl_2N_6O_2Pt$: C 51.49, H 7.56, N 9.01, Found C 51.37, H 7.55, N 8.98; MS (MALDI): *m/z* calcd. 933.0, found 933.4 $[M+H]^+$.

Synthesis of G. The synthesis of **G** was carried out using a procedure described previously.[24b] ^{1}H NMR (400 MHz, DMSO-d_6) δ 7.33 (1H, s, Ar*H*), 7.14 (3H, m, Ar*H*), 6.12 (2H, s, $ArC(CH_3)_2$ N*H*), 5.82 (2H, t, *J* = 5.8 Hz, - $N\mathit{H}CH_2$-), 3.75 (12H, q, *J* = 6.9 Hz, -$OC\mathit{H}_2$-), 2.90 (4H, q, *J* = 5.9 Hz, -$NHC\mathit{H}_2$-), 1.51 (12H, s, Ar-$C(C\mathit{H}_3)_2$-), 1.38 (4H, quin, *J* = 7.5 Hz, -$CH_2C\mathit{H}_2CH_2$-), 1.15 (18H, t, *J* = 6.9 Hz, -$CH_2C\mathit{H}_3$), 0.51 (4H, t, *J* = 8.1 Hz, -$C\mathit{H}_2$Si); Anal. calcd. for $C_{32}H_{62}N_4O_8Si_2$: C 55.94, H 9.10, N 8.15, Found C 56.01, H 9.01, N 8.11; MS (ESI): *m/z* calcd. 709.4, found 709 $[M+Na]^+$.

ASSOCIATED CONTENT

Supporting Information.
Experimental details, NMR spectra, solubility chart, SEM, XRPD and crystallographic data in tabular and in CIF format for the DMA solvate of cisplatin. CCDC 1406192. This material is available free of charge via the Internet at http://pubs.acs.org.

AUTHOR INFORMATION

Corresponding Authors

* jon.steed@durham.ac.uk; arnabdawn16@gmail.com

NOTES

The authors declare no competing financial interest.

ACKNOWLEDGMENT

We are grateful for support from the European Union Marie Curie International Incoming Fellowship (PIIF-GA-2012-326487–GELCRYS) to A. Dawn.

† Dedicated to Prof. Manfred Scheer on occasion of his 60th Birthday.

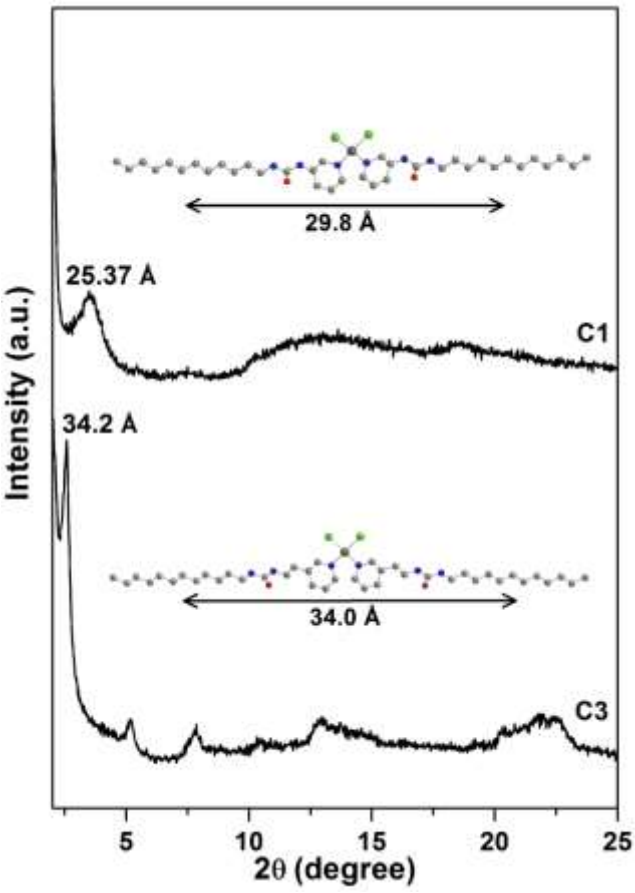

Figure 7. XRPD patterns of the dried samples prepared from gels of **C1** and **C3** in *o*-xylene (2% w/v), together with the molecular spacing assigned using an extended conformation (with partial energy minimization) for both the compounds. A 50% of the length of a dodecyl chain is approximated as ordered, considering the high flexibility of the terminal part of the chain.

REFERENCES

1. (a) Hilfiker, R. Polymorphism: In the Pharmaceutical Industry; Wiley-VCH: Weinheim, **2006**. (b) *Solid State Characterization of Pharmaceuticals*; Storey, R. A.; Ymén, I., Eds.; Wiley: Chichester, 2011. (c) Bernstein, J. *Crystal Growth and Design* **2011**, *11*, 632. (d) Byrn, S.; Pfeiffer, R.; Gany, M.; Hoiberg, C.; Poochikian, G. *Pharm. Res.* **1995**, *12*, 945.

2. (a) Blagden, N.; de Matas, M.; Gavan, P. T. ; York, P. *Adv. Drug Deliv. Rev.* **2007**, *59*, 617. (b) Steed, J. W. *Trends Pharm. Sci.* **2013**, *34*, 185. (c) Bernstein, J. *Polymorphism in Molecular Crystals*; Clarendon Press: Oxford, 2002. (d) *Polymorphism in Pharmaceutical Solids*; 1st ed.; Brittain, H. G., Ed.; Marcel Dekker Inc.: New York, 1999. (e) *Pharmaceutical Salts and Co-crystals*; Wouters, J.; Quéré, L., Eds.; Royal Society of Chemistry: Cambridge, 2012.

3. Ostwald, W. *Z. Phys. Chem.* **1897**, *22*, 289.

4. Bauer, J.; Spanton, S.; Henry, R.; Quick, J.; Dziki, W.; Porter, W.; Morris, J. *Pharm. Res.* **2001**, *18*, 859.

5. Aguiar, A. J.; Krc, J.; Kinkel, A. W.; Samyn, J. C. *J. Pharm. Sci.* **1967**, *56*, 847.

6. "Guideline for Submitting Supporting Documentation in Drug Applications for the Manufacture of Drug Substances," U.S. Department of Health and Human Services, Food and Drug Administration, Center for Drug Evaluation and Research, February 1987.

7. Adhiyaman, R; Basu, S. K. *Int. J. Pharm.* **2006**, *321*, 27.

8. (a) Armington, A. F.; O′Connor, J. J. *Inorg. Synth.* **1980**, *20*, 1. (b) Cudney, B.; Patel, S.; McPherson, A. *Acta Cryst.* **1994**, *D50*, 479. (c) Sugiyama, S.; Shimizu, N.; Sazaki, G.; Hirose, M.; Takahashi, Y.; Maruyama, M.; Matsumura, H.; Adachi, H.; Takano, K.; Murakami, S.; Inoue, T.; Mori, Y. *Cryst. Growth Des.* **2013**, *13*, 1899. (d) Duffus , C.; Camp, P. J., Alexander, A. J. *J. Am. Chem. Soc.* **2009**, *131*, 11676.

9. (a) Terech, P.; Weiss, R. G. *Chem. Rev.* **1997**, *97*, 3133. (b) Sangeetha, N. M.; Maitra, U. *Chem. Soc. Rev.* **2005**, *34*, 821. (c) Dastidar, P. *Chem. Soc. Rev.* **2008**, *37*, 2699. (d) Hirst, A. R.; Escuder, B., Miravet, J. F.; Smith, D. K. *Angew. Chem., Int. Ed.* **2008**, *47*, 8002. (e) Piepenbrock, M-O. M.; Lloyd, G. O.; Clarke, N.; Steed, J. W. *Chem. Rev*. **2010**, *110*, 1960. (f) Dawn, A.; Shiraki, T.; Haraguchi, S.; Tamaru, S-i.; Shinkai, S. *Chem. Asian J.* **2011**, *6*, 266. (g) Buerkle, L. E.; Rowan, S. J. *Chem. Soc. Rev*. **2012**, *41*, 6089. (h) Yu, G.; Yan, X.; Han, C.; Huang, F. *Chem. Soc. Rev.* **2013**, *42*, 6697 (i) Babu, S. S.; Praveen, V. K.; Ajayaghosh, A. *Chem. Rev.* **2014**, *114*, 1973. (j) Feng, Y.; He, Y-M.; Fan, Q-H. *Chem. Asian J.* **2014**, *9*, 1724.

10. Aparicio, F.; Matesanz, E.; Sánchez, L. *Chem. Commun.* **2012**, *48*, 5757.

11. (a) Kumar, D. K.; Steed, J. W. *Chem. Soc. Rev.* **2014**, *43*, 2080. (b) Diao, Y.; Whaley, K. E.; Helgeson, M. E.; Woldeyes, M. A.; Doyle, P. S.; Myerson, A. S.; Hatton, T. A.; Trout, B. L. *J. Am. Chem. Soc.* **2012**, *134*, 673. (c) Pauchet, M.; Morelli, T.; Coste, S.; Malandain, J.-J.; Coquerel, G. *Cryst. Growth Des.* **2006**, *6*, 1881.

12. (a) Hartgerink, J. D.; Beniash, E.; Stupp, S. I. *Science* **2001**, *294*, 1684. (b) Estroff, L. A.; Addadi, L.; Weiner, S.; Hamilton, A. D. *Org. Biomol. Chem.* **2004**, *2*, 137.

13. Foster, J. A.; Piepenbrock, M-O. M.; Lloyd, G. O.; Clarke, N.; Howard, J. A. K.; Steed, J. W. *Nature Chem.* **2010**, *2*, 1037.

14. Henisch, H. K. *Crystal Growth in Gels*; The Pennsylvania State University Press: University Park, PA, 1976.

15. Arlin, J-B.; Price, L. S.; Price, S. L.; Florence, A. J. *Chem. Commun.* **2011**, *47*, 7074.

16. (a) Flechon, A.; Culine, S.; Droz, J-P. *Crit. Rev. Oncol. Hematol.* **2001**, *37*, 35. (b) Wheate, N. J.; Walker, S.; Craig, G. E.; Oun, R. *Dalton. Trans.* **2010**, *39*, 8113.

17. Milburn, G. H.W.; Truter, M. R. *J. Chem. Soc. A* **1966**, 1609.

18. Kaplan, M. A.; Granatek, A. P. *US 4322391*, **1982**.

19. Ting, V. P.; Schmidtmann, M.; Wilson, C. C.; Weller, Mark T. *Angew. Chem. Int. Ed.* **2010**, *49*, 9408.

20. (a) Raudaschl, G.; Lippert, B.; Hoeschele, J. D.; Howard-Lock, H. E.; Lock, C. J. L.; Pilon, P. *Inorg. Chim. Acta* **1985**, *106*, 141. (b) Johnston, D. H.; Miller, N. A.; Tackett, C. B. *Acta. Cryst.* **2012**, *E68*, m863.

21. Alston, D. R.; Stoddart, J. F.; Williams, D. J. *J. Chem. Soc., Chem. Commun.* **1985**, 532.

22. Lewis, J. E. M.; Gavey, E. L.; Cameron, S. A.; Crowley, J. D. *Chem. Sci*. **2012**, *3*, 778.

23. For metallogels see: (a) Beck, J. B.; Rowan, S. J. *J. Am. Chem. Soc.* **2003**, *125*, 13922. (b) Zhang, J; Su, C-Y. *Coord. Chem. Rev.* **2013**, *257*, 1373. (c) Miao, W.; Zhang, L.; Wang, X.; Cao, H.; Jin, Q.; Liu, M. *Chem. Eur. J*. **2013**, *19*, 3029; (d) Miao, W.; Zhang, L.; Wang, X.; Qin, L.; Liu, M. *Langmuir* **2013**, *29*, 5435. (e) Lin Q.; Lu T-T.; Zhu, X.; Sun, B.; Yang, Q-P.; Wei, T-B; Zhang, Y-M. *Chem. Commun.* **2015**, *51*, 1635.(f) Tam, A. Y.-Y.; Yam, V. W.-W. *Chem. Soc. Rev.* **2013**, *42*, 1540.(g) Fages, F. *Angew. Chem., Int. Ed. Engl.* **2006**, *45*, 1680.

24. For bis(urea) gels see: (a) Steed J. W. *Chem. Soc. Rev.* **2010**, *39*, 3686. (b) Piepenbrock, M-O. M.; Clarke, N.; Foster, J. A.; Steed, J. W. *Chem. Commun.* **2011**, *47*, 2095. (c) Lloyd, G. O.; Piepenbrock, M-O. M.; Foster, J. A.; Clarke, N.; Steed, J. W. *Soft Matter* **2012**, *8*, 204. (d) Foster, J. A.; Edkins, R. M.; Cameron, G. J.; Colgin, N.; Fucke, K.; Ridgeway, S.; Crawford, A. G.; Marder, T. B.; Beeby, A.; Cobb, S. L.; Steed, J. W. *Chem. Eur. J*. **2014**, *20*, 279. (e) de Loos, M.; Friggeri, A.; van Esch, J.; Kellogg, R. M.; Feringa, B. L. *Org. Biomol. Chem.* **2005**, *3*, 1631. (f) de Loos, M.; Ligtenbarg, A. G. J.; van Esch, J.; Kooijman, H.; Spek, A. L.; Hage, R.; Kellogg, R. M.; Feringa, B. L. *Eur. J. Org. Chem.* **2000**, 3675. (g) van Esch, J. H.; Schoonbeek, F.; de Loos, M.; Kooijman, H.; Spek, A. L.; Kellogg, R. M.; Feringa, B. L. *Chem. Eur. J.* **1999**, *5*, 937. (h) George, M.; Tan, G.; John, V. T.; Weiss, R. G. *Chem.-Eur. J.* **2005**, *11*, 3243.

25. Arai S.; Imazu, K.; Kusuda, S.; Yoshihama, I.; Tonegawa, M.; Nishimura, Y.; Kitahara, K-i.; Oishi, S.; Takemura, T. *Chem. Lett.* **2006**, *35*, 634.

26. (a) Tessier, C.; Rochon, F. D. *Inorg. Chim. Acta* **1999**, *295*, 25. (b) Still, B. M.; Kumar, P. G. A.; Aldrich-Wright, J. R.; Price, W. S. *Chem. Soc. Rev.* **2007**, *36*, 665.

27. (a) Hartley, F. R. *Chem. Soc. Rev.* **1973**, 2, 163. (b) Anderson, K. M.; Orpen, A. G. *Chem. Commun.* **2001**, 2682.

28. The temperature dependent NMR studies of **C2** in EtOH-d_6 remained inconclusive because of shimming difficulties from the opaque solution even at a low concentration.

29. Schneider, H.-J.; Yatsimirsky, A. *Principles and Methods in Supramolecular Chemistry*; John Wiley & Sons: Chichester, 1999.

30. Petrova, R. I.; Patel, R.; Swift, J. A. *Cryst. Growth Des.* **2006**, *6*, 2709.

31. Single crystal X-ray data for DMA solvate of cisplatin: formula $2[PtCl_2(NH_3)_2].C_4H_9NO$, M = 687.24 $gmol^{-1}$, triclinic space group P$\bar{1}$, a = 6.2421(2) Å, b = 10.1937(3) Å, c = 12.9498(3) Å, α = 108.616(2)^o, β = 91.868(2)^o, γ = 95.517(2)^o, V = 775.52(4) $Å^3$, Z=2, ρ_{calc} = 2.943 g/cm^3, μ = 18.698 mm^{-1}, R_1 = 0.032 (I > 2σ(I)), wR_2 = 0.0552 (all data), F(000) = 624.0.

32. (a) Connick, W. B.; Henling, L. M.; Marsh, R. E.; Gray, H. B. *Inorg. Chem.* **1996**, *35*, 6261. (b) Martin, D. S.; Hunter, L. D.; Kroening, R.; Coley, R. F. *J. Am. Chem. Soc.* **1971**, *93*, 5433.

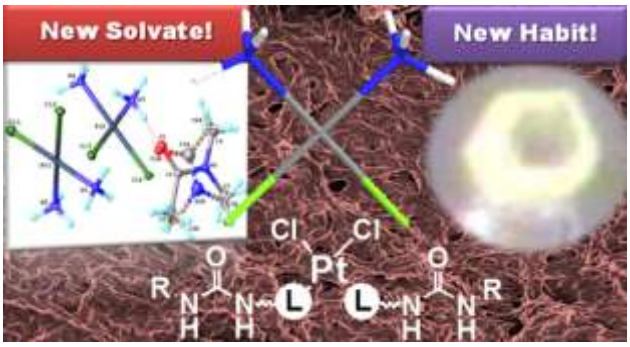

A targeted supramolecular gel designed to mimic cisplatin allows the characterization of a novel solvate and new crystal habit